JOURNAL OF MATERIALS SCIENCE **34** (1999) 4573–4578

Optical and structural properties of (Ba, Sr)TiO_3 thin films grown by radio-frequency magnetron sputtering

Y. P. WANG, T. Y. TSENG
Department of Electronic Engineering and Institute of Electronics, National Chiao-Tung University, Hsinchu, Taiwan, Republic of China
E-mail: tseng@cc.nctu.edu.tw

We studied the structural and optical properties of (Ba, Sr)TiO_3 (BST) films deposited on the transparent substrates at various temperatures of 350–650 °C and annealed at 450–650 °C. Improved crystallization can be observed on 650 °C annealed film whose substrate temperature is 350 °C. The refractive index increased from 2.17 to 2.59 at $\lambda = 410$ nm for the BST films deposited at 350–650 °C and it varied from 2.17 to 2.25 after annealing up to 650 °C. In addition, the refractive-index dispersion data related to the short-range-order structure of BST films obeyed the single-oscillation energy model. The indirect energy gap of the films deposited on Al_2O_3 and quartz substrates was found to be about 3.5 eV. According to the analysis of reflectance data, the optical inhomogeneity of films can be reduced by depositing the films at intermediate temperatures 450–550 °C.

1. Introduction

At present, ferroelectric thin films have received much attention for fabricating novel functional devices [1–6]. In particular, the ferroelectric films are expected to be excellent in realization of various optical-applications due to their wide energy gap (>3 eV), large static dielectric constant, high refractive index and low absorption coefficient. The optical properties of the epitaxial PLT thin films grown on MgO and Al_2O_3 substrates have been investigated [7]. Zhu *et al.* [8] studied the film-size effect on the optical energy gap of $BaTiO_3$. The (Ba, Sr)TiO_3 (BST) films, conrast to above mentioned ferroelectric materials, can display paraeletric phase by controlling Ba/Sr ratio and perform a high transparency as an insulating layer of an electroluminescent devices [9]. The current research on the optical properties of BST should attract more interests due to its potential applications in flat panel displays and integrated optics.

In this study, the BST thin films were prepared on the transparent substrates by rf-sputtered at substrate temperatures 350–650 °C. We investigated the effect of substrate temperature on the structure and optical properties of BST films. On the basis of single-oscillator model [10], the parameters related to the short-range-order structure were analyzed.

2. Experimental

BST films were sputtered on the clean Corning 7059 glass, fused-quartz and $(1\bar{1}02)$-oriented Al_2O_3 by a magnetron radio-frequency sputtering system. The $(Ba_{0.7}Sr_{0.3})TiO_3$ target of 2 in. diameter and 0.125 in. thickness was fabricated using standard solid-state process. An operating pressure of 40 mTorr was maintained by a mixture of high-purity argon and oxygen at a flow ratio of 20/1. All films were deposited at a fixed radio-frequency power of 80 W for 2.5 h and the substrate temperature was varied from 350 to 650 °C using a quartz halogen lamp. Post-annealing of the 350 °C-deposited film was carried-out in an argon atmosphere for 2 h at temperatures ranging from 450 to 650 °C. The film crystal structures were examined using X-ray diffraction (XRD, Siemens D5000) with CuK_α radiation. The optical transmittance and reflectance of BST films were measured in the wavelength range of 250–900 nm using double beam spectrophotometer (Hitachi model U3410 UV-Vis-NIR). The optical constant and film thickness were calculated on the basis of the envelope technique and interference-fringe equation [11]. The film thickness was also cross-checked from the fracture surface of the film by scanning electron microscope (SEM, Hitachi, S-4000).

3. Results and discussion

Fig. 1a displays XRD patterns of the films deposited on Corning substrates at various substrate temperatures ranging from 350 to 650 °C. The intensities of (100), (110) and (200) peaks were enhanced with the increasing substrate temperature, indicating that better crystallinity can be obtained at higher substrate temperatures. Fig. 1b revealed that the crystallization of 350 °C-deposited film can be improved by subsequent annealing at 650 °C.

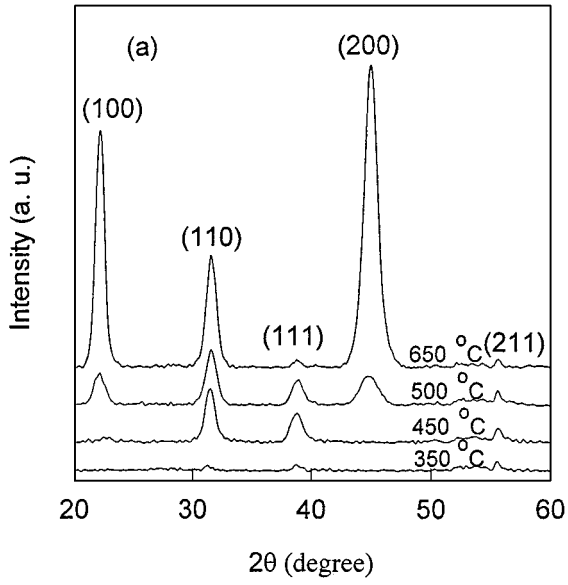

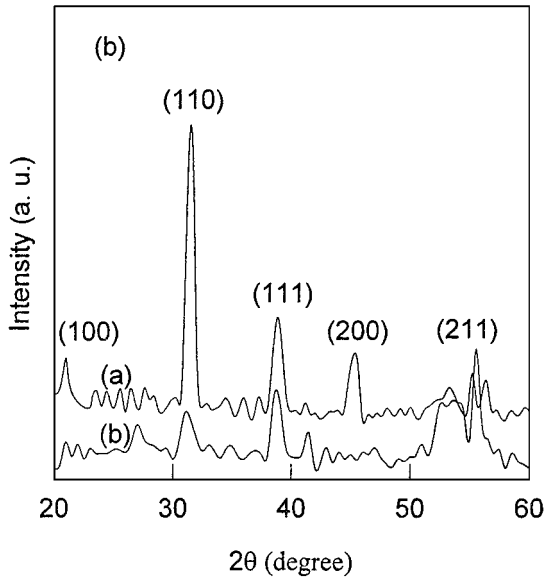

Figure 1 (a) XRD patterns of BST films deposited on Corning substrates at various substrates temperatures indicated (b) XRD patterns of BST films deposited on Corning substrates at 350 °C (i) and followed by annealing at 650 °C (ii).

Fig. 2 depicts the spectral transmittance characteristic of bare Corning substrate and the BST films deposited on it at various substrate temperatures. The interference fringes are a result of the interference between the air-film and film-substrate interfaces. The refractive index (n) was derived by employing the envelope method [11] on the basis of the following expressions:

$$n = \left[N + \left(N^2 - n_s^2\right)^{1/2}\right]^{1/2} \quad (1)$$

$$N = 2n_s\left(\frac{1}{T_{min}} - \frac{1}{T_{max}}\right) + \frac{n_s^2 + 1}{2} \quad (2)$$

in which T_{max} and T_{min} are the corresponding transmittance maximum and minimum at a certain wavelength λ, one being measured and the other calculated; n_s is the refractive index of Corning glass substrate ($\approx$1.51). Fig. 3 displays the calculated refractive index (n) as a function of wavelength (λ) for various substrate temperatures. The refractive index increased from 2.17 to 2.59 (at $\lambda = 410$ nm) as temperature increased from 350 to 650 °C. The behavior of n vs. λ can be fitted into a formula [11], $n = A + \frac{B}{\lambda} + \frac{C}{\lambda^2}$, as shown by solid lines in Fig. 3. The dependence of n on substrate temperature was consistent with those normally observed in many oxides [12–15]. The increase of the refractive index of the films deposited at higher temperature may be attributed to an increase in packing density, crystallization and also to the oxygen deficiency [12–15].

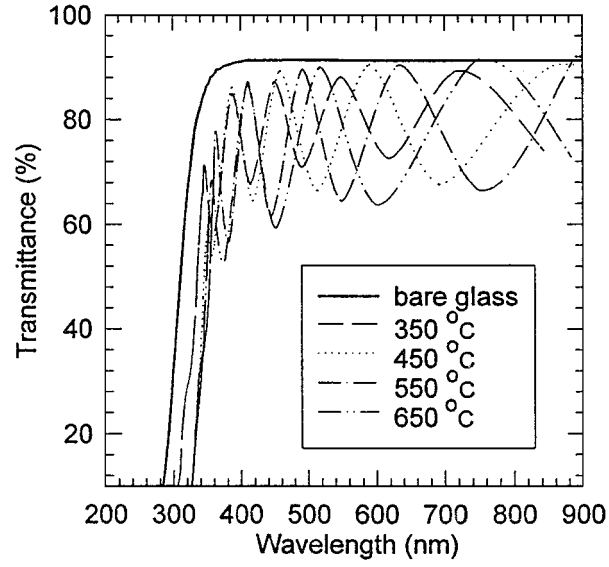

Figure 2 Transmittance spectra as a function of wavelength for BST films deposited at various substrate temperatures.

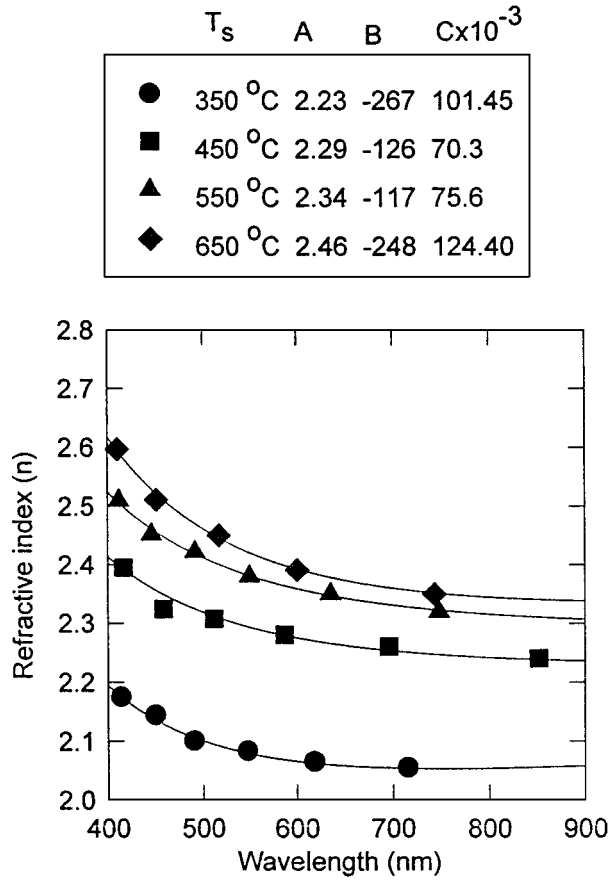

Figure 3 Variation of refractive index as a function of wavelength deposited at various substrate temperatures for 2.5 h.

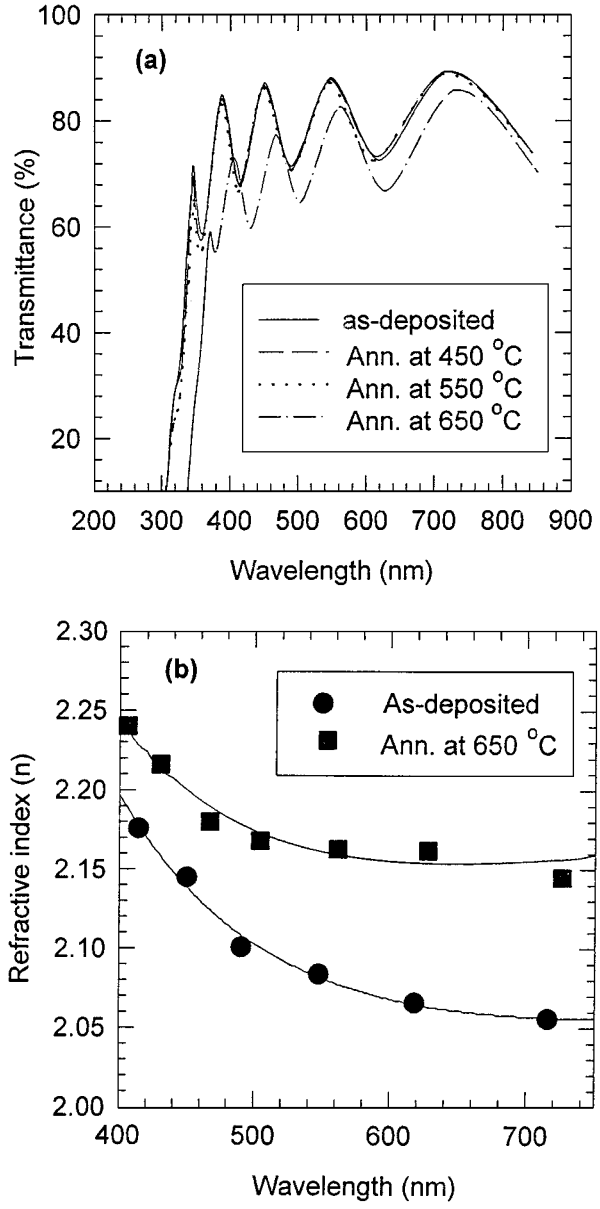

Figure 4 (a) Transmittance spectra as a function of wavelength for the as-deposited (=350 °C) and subsequently annealed BST films. (b) Variation of refractive index as a function of wavelength for the as-deposited and annealed BST films.

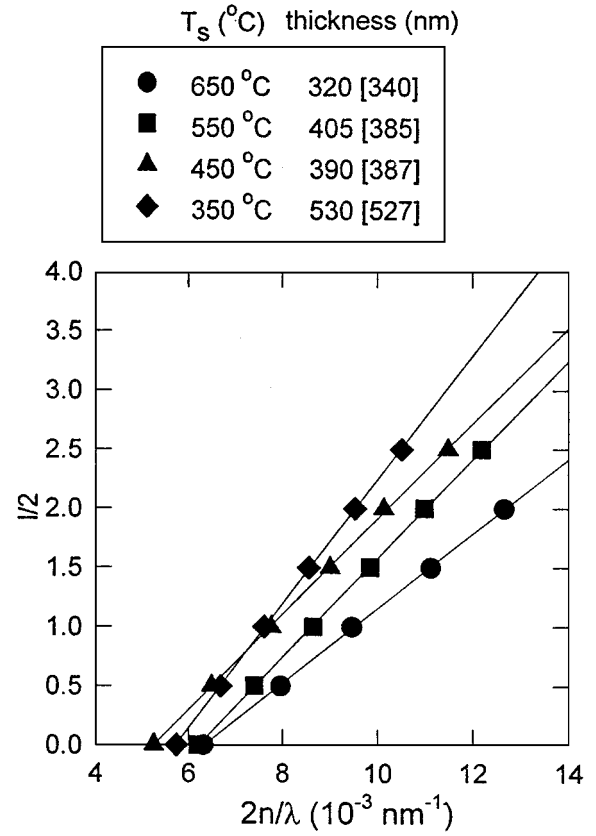

Figure 5 Plot of $(m/2)$ vs. $(2n/\lambda)$ for the BST films deposited at various substrate temperatures to obtain film thickness. The number in ( ) represents the thickness observed by SEM.

Fig. 4a depicts no significant change in transmittance maxima and minima for the films annealed at lower temperatures whereas transmittance maxima and minima decreased and the interference pattern shift toward a longer wavelength region in the 650 °C annealed film. Fig. 4b shows the variation of refractive index as a function of wavelength for the film deposited at 350 °C and subsequently annealed at 650 °C. The lower transmittance after 650 °C annealing may be mainly due to the strong scattering of the light in the film caused by some discernible microcracks arising from mismatched thermal expansion of the film and substrate. Suhail *et al.* [12] found that the TiO_2 film deposited at room temperature, after annealing at 700 °C, showed an increased refractive index, $(\Delta n/n) = +7.3\%$ at 550 nm, a thickness reduction of -20% and a shift in the spectral pattern to a lower wavelength region ($\Delta\lambda_m/\lambda_m < 0$) resulting from the effect of interference fringe, $2nd = m\lambda$. Our result for the annealing of BST film with $\Delta n/n = +3.9\%$ at $\lambda = 550$ nm and $\Delta\lambda_m/\lambda_m > 0$ revealed a lesser thickness reduction after annealing at 650 °C.

Fig. 5 indicates the least-square fit of the measured refractive index vs. wavelength by the interference-fringe relation [11],

$$\frac{m}{2} = d\left(\frac{2n}{\lambda}\right) - k, \quad m = 0, 1, 2, \ldots \tag{3}$$

in which k is the order number of the observable first extreme ($m = 0$) of the spectrum. The film thickness can be obtained from the slope of the plot shown in Fig. 5. These thickness is in good agreement with those (numbers indicated in [ ] of Fig. 5), which were observed by SEM.

According to the single-oscillation model [10], the refractive index as a function of wavelength can be expressed as:

$$n^2 - 1 = \frac{E_o E_d}{E_o^2 - \left(\frac{hc}{\lambda}\right)^2} \tag{4}$$

where c is the light speed, h Planck constant, E_o the single-oscillator energy and E_d the dispersion energy. The E_o and E_d values can be obtained from the intercept and slope of the plot $(n^2 - 1)^{-1}$ vs. λ^{-2}, respectively. Fig. 6 exhibits a sufficient extended region of linearity which can be employed to determine E_o and E_d. At long

TABLE I The fitting parameters obtained from the single-oscillation model for BST films deposited at various substrate temperatures

Substrate temperature T_s (°C)	Single oscillation energy E_o (eV)	Dispersion energy E_d (eV)	Empirical ratio β (eV)
350	6.89	20.61	0.214
450	6.69	26.14	0.272
550	6.42	26.33	0.274
650	5.87	24.48	0.255

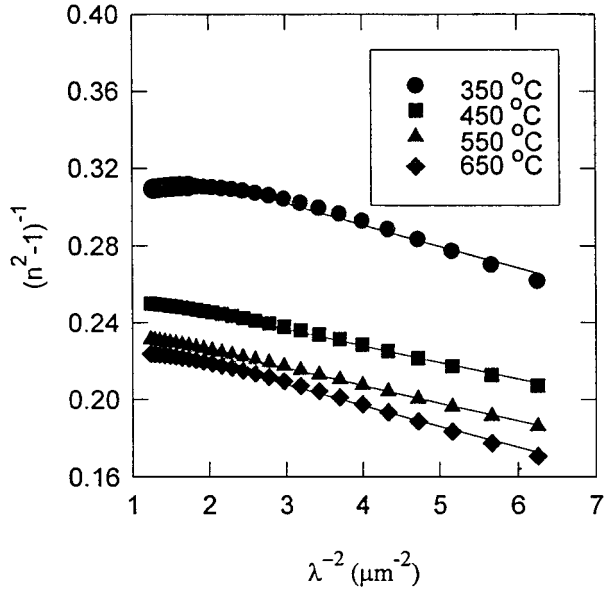

Figure 6 Plots of refractive-index factor $(n^2-1)^{-1}$ vs. λ^{-2} for the BST films deposited at various substrate temperatures.

wavelengths region, a curvature deviation from linearity is usually observed due to negative contribution of lattice vibrations to the refractive index [10]. The corresponding E_o, as summarized in Table I, decreases with increasing substrate temperature whereas E_d (=24.48 eV) at higher substrate temperature 650 °C is close to the E_d of pure bulk $BaTiO_3$ ($E_d = 23.3$ eV) and $SrTiO_3$ ($E_d = 23.32$ eV) materials [10]. Structure should play an influential role for oscillation and dispersion energies. For lower temperature deposited films, a small amount of amorphous phase would result in higher E_o value. Table I also includes the values of $\beta = E_d/(N_c Z_a N_e)$ [10], where N_c (=6) is the coordinate number of cation nearest neighbor to the anion, Z_a (=2) the chemical valency of the anion and N_e (=8) the effective number of valence electrons per anion. The observed β values in our cases are coincident with the empirical values given by $\beta \approx 0.26 \pm 0.04$ eV, which was followed by many bulk oxides [10].

Fig. 7a displays the transmittance spectra of BST films deposited on Al_2O_3 ($n_s = 1.80$) and fused-quartz ($n_s = 1.51$) substrates. The low-wavelength absorption of bare Al_2O_3 and quartz substrates is much weaker than that of bare corning substrate. Their refractive index as a function of wavelength is shown in Fig. 7b. The low-wavelength absorption data for BST films prepared on Al_2O_3 and quartz substrates is related to the fundamental absorption which refers to the band-to-band transi-

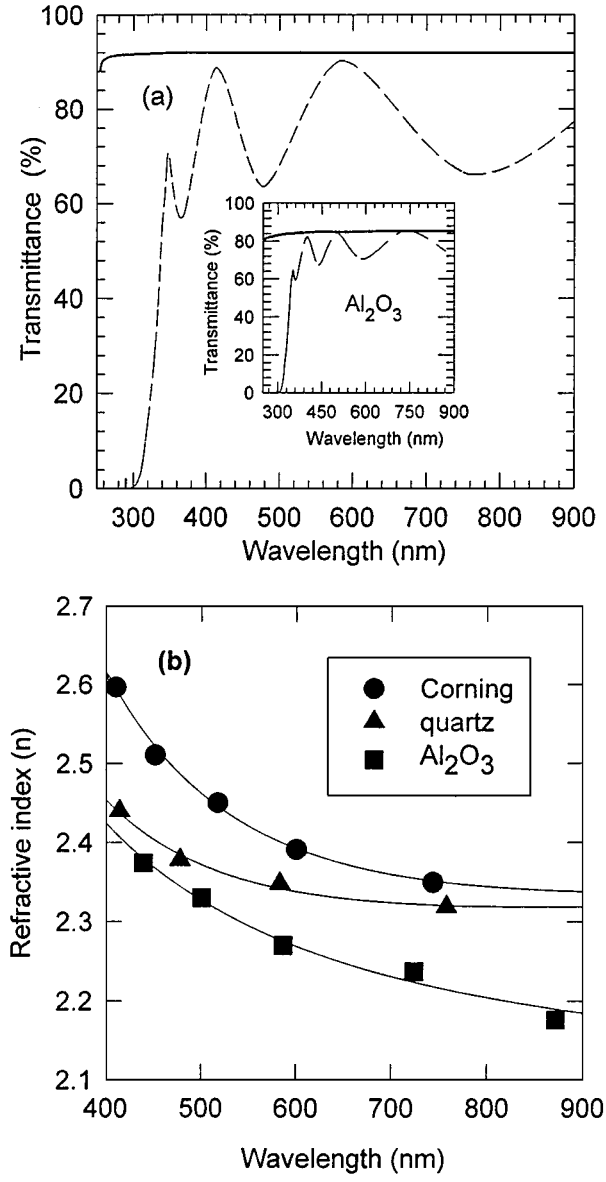

Figure 7 (a) The transmittance spectra of bare quartz substrate and 650 °C. The insert plot displayed transmittance spectra of bare Al_2O_3 substrate and BST films deposited on it, and (b) Variation of refractive index as a function of wavelength for BST films prepared on various substrates.

tion, i.e., to the excitation of an electron from the valence band to the conduction band. The BST energy gap can be obtained from the following equations [16, 17]:

$$\alpha h\nu = \text{constant} \times (h\nu - E_g)^2 \tag{5}$$

where $h\nu$ is the photon energy, E_g the optical energy gap of allowed indirect and direct transition. The absorption coefficient, α is given as [17]

$$\alpha = \frac{\ln\left(\frac{1}{T}\right)}{d} \tag{6}$$

in which T the transmittance and d the film thickness.

The $(\alpha h\nu)^{1/2}$ vs. $h\nu$ plots for the films on Al_2O_3 and quartz substrates as represented by Equation 5 show good linearity at wavelength below 400 nm, as shown in Fig. 8. The plots of $(\alpha h\nu)^{1/2}$ vs. $h\nu$ were found not to be straight lines over any part of the absorption spectra,

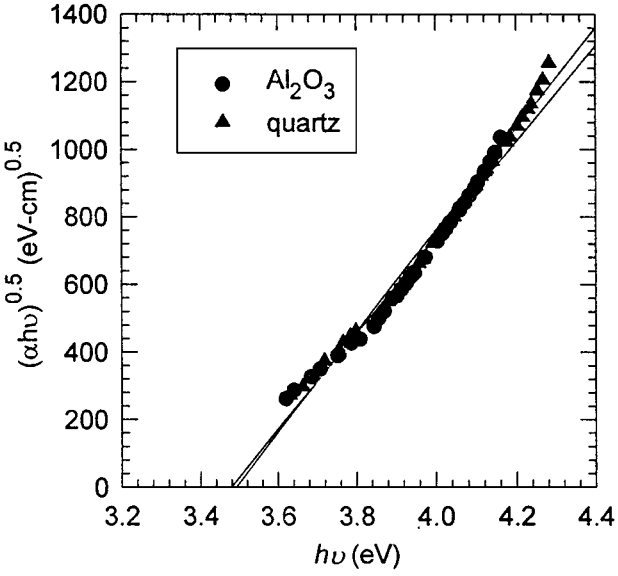

Figure 8 Plot of $(\alpha h\nu)^{1/2}$ vs. $h\nu$ for BST films deposited on Al_2O_3 and fused quartz substrates.

thus supporting the model of indirect band gap for the deposited films. By extrapolating the linear portion of these curves to zero absorption, the calculated energy gaps were about 3.5 eV which are close to the energy gaps of $BaTiO_3$ films (3.6–4.1 eV) [8, 18] and $SrTiO_3$ ceramic (=3.43 eV) [19]. The reduced energy gap of (Ba, Sr)TiO_3 might be due to the Sr in the Ba site substitution.

The optical inhomogeneity of the films was analyzed by using the near normal reflectance of the films and the bared substrate surface. The inhomogeneous refractive index (Δn) along the film thickness was determined using the empirical relation [20]:

$$\Delta n = n_o - n_i = n_{av}\frac{R_f - R_s}{4.4R_s} \tag{7}$$

The n_o in Equation 7 is the refractive index at the air-film interface, n_i at the film-substrate interface and n_{av} the average index of the film. R_s and R_f are the reflectance at the front surface of the substrate and films, respectively. Both R_s and R_f can be computed from the measured reflectance of the bare and deposited substrate, R_{so} and R_{fo}, using the following expressions [21]:

$$R_{so} = \frac{2R_s}{1 + R_s} \tag{8}$$

$$R_{fo} = R_f + \frac{R_s(1 - R_f)^2}{(1 - R_sR_f)} \tag{9}$$

where Δn can be positive or negative according to the gradation in the film [20]. Negative Δn value indicates that the refractive index decreases from substrate to the top surface of the film and vice versa. The degree of inhomogeneity of the films, $\Delta n/n_{av}$, calculated from the points of reflectance minima around 600–700 nm, where the R_{so} (R_s) is almost independent of λ, as shown in Fig. 9 and Table II, was found to vary from −7.3 to −4.3% as the substrate temperature was increased from 350 to 650 °C. The optical homogeneity of BST films was found to be better for the films deposited at intermediate temperatures 450–550 °C.

TABLE II Optical inhomogeneity analysis for the films deposited at various temperatures

Substrate temperature (°C)	Wavelength (nm)	$\Delta n/n_{av}$ (%)
350	715	−7.3
450	593	−3.3
550	630	−3.7
650	739	−4.3

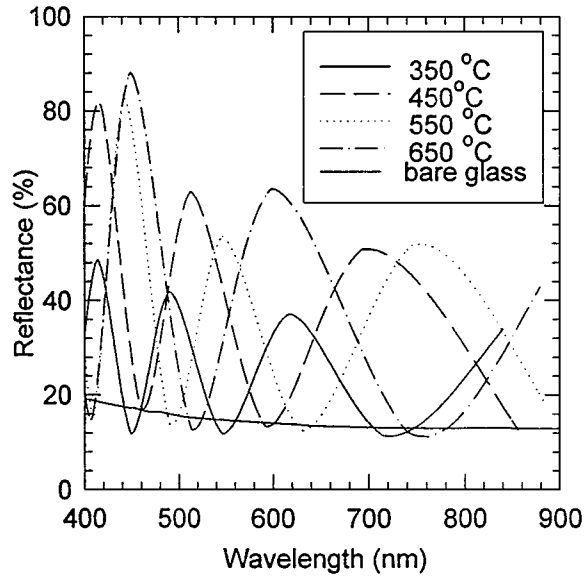

Figure 9 Observed reflectance spectra as a function of wavelength for bare substrate (R_{so}) and BST films (R_{fo}) deposited at various substrate temperatures.

4. Conclusions

We have studied the effect of various substrate temperatures as well as post annealing on the structural and optical properties of BST films prepared by rf magnetron sputtering. Crystallization sets in at the deposited films and it is further improved by post-deposition annealing at 650 °C, as observed from X-ray results. The refractive index of the films were increased with an increased substrate temperature. The film thickness calculated from interference-fringe equation is in good agreement with the one observed by scanning electron microscope. The dependence of refractive index on the wavelength obeys the single-oscillation model, from which the parameters E_o, E_d and β were determined and were consistent with the experimental values for most oxides. The energy gap of the deposited films on various substrates was found to be around 3.5 eV of indirect-transition type. The film deposited at 350 °C was more inhomogeneous whereas it has better optical homogeneity when deposited at intermediate substrate temperature.

Acknowledgement

This work was support from the National Science Council of Republic of China under project no. NSC 86-2112-M009-028.

References

1. T. MATSUKI, Y. HAYASHI and T. KUNIO, *IEDM-95* (1996) 691.
2. M. H. SONG, Y. H. LEE, T. S. HANN and M. H. OH, *J. Appl. Phys.* **79** (1996) 3744.
3. K. OKAMOTO, Y. NASU and Y. HAMAKAWA, *IEEE Trans. Electron Devices ED-28* (1991) 698.
4. A. YUUKI, M. YAMAMUKA, T. MAKITA, T. HORIKAWA, T. SHIBANO, N. HIRANO, H. MAEDA, N. MIKAMI, K. ONO, H. OGATA and H. ABE, *IEEE IEDM-95* (1995) 115.
5. Y. P. WANG and T. Y. TSENG, *J. Appl. Phys.* **81** (1997) 6762.
6. A. KINGON, S. K. STREIFFER, C. BASCERI and S. R. SUMMERFELT, *MRS Bulletin* (1996) 46.
7. Y. KIM and A. ERBIL, *Appl. Phys. Lett.* **70** (1997) 143.
8. J. S. ZHU, X. M. LU, W. JIANG, W. TIAN, M. ZHU, M. S. ZHANG, X. B. CHEN, X. LIU and Y. N. WANG, *J. Appl. Phys.* **81** (1997) 1392.
9. T. S. KIM, M. H. OH and C. H. KIM, *Jpn. J. Appl. Phys.* **32** (1993) 2837.
10. S. H. WEMPLE and M. DIDOMENICO, *Phys. Rev. B* **3** (1971) 1338.
11. R. SWANEPOEL, *J. Phys. E, Sci. Instrum.* **16** (1983) 1214.
12. M. H. SUHAIL, G. M. RAO and S. MOHAN, *J. Appl. Phys.* **71** (1992) 1421.
13. M. G. KRISHNA, K. N. RAO, M. A. MURTHY and S. MOHAN, *J. Mater. Sci. Eng.* **B 5** (1990) 427.
14. M. MESBAH, A. BOYER and E. GROUBERT, *ibid.* **27** (1992) 83.
15. H. KUSTER and J. EBERT, *Thin Solid Films* **70** (1980) 43.
16. S. R. ELLIOTT, "Physics of Amorphous Materials" (John Wiley & Sons, New York, 1990) p. 328.
17. E. A. DAVIS and N. F. MOTT, *Phil. Mag.* **22** (1970) 903.
18. A. MANSINGH and C. V. R. VASANTA, *J. Mater. Sci. Lett.* **7** (1988) 1104.
19. M. N. KAMALASANAN, N. D. KUMAR and S. CHANDRA, *J. Appl. Phys.* **74** (1993) 679.
20. D. P. ARNDT, R. M. AZZAM, J. M. BENNETT, J. P. BORGONO, C. K. CARNUGLIA, W. E. CASE, J. A. DOBROWOLSKI, U. J. GIBSON, T. T. HART, F. C. HO, V. A. HODGIN, W. R. KLAPP, H. A. MACLEOD, E. PELLETIER, M. K. PURVIS, D. M. QUINN, D. H. STOME, R. SWENSON, P. A. TEMPLE and T. F. THOUN, *Appl. Opt.* **23** (1984) 3571.
21. R. JACOBSSON, *Arkiv Fys.* **24** (1963) 17.

Received 24 November 1997
and accepted 10 March 1999